Induced anisotropy in amorphous Co-Zr-M (M =Zr,Nb,Ti) and Co-Zr-Pt thin films: A magnetic and a structural study

G. Suran
Laboratoire de Magnétisme, 1 place A. Briand, 92195 Meudon CEDEX, France

F. Machizaud
Laboratoire de Magnétisme, 1 place A. Briand, 92195 Meudon CEDEX, France
and Laboratoire de Métallurgie, Ecole des Mines de Nancy, 54042 Nancy CEDEX, France

M. Naili
Laboratoire de Magnétisme, 1 place A. Briand, 92195 Meudon CEDEX, France
(Received 18 February 1992; revised manuscript received 12 November 1992)

A magnetic and structural investigation was carried out on $Co_{95-x}Zr_5M_x$ (M=Zr, Nb, or Ti) and $Co_{91-x}Zr_9Pt_x$ amorphous thin films in order to determine the physical origin of the induced in-plane uniaxial anisotropy K_u. The films were prepared by rf sputtering and the deposition was performed in a magnetic field. The variations of K_u were studied as a function of the sputtering parameters, composition, concentration, the thermomagnetic treatment, and structural-relaxation process. As a result of these investigations a model for the origin of K_u is advanced, which involves the single-ion anisotropy mechanism. K_u is the sum of two contributions $K_u^a+K_u^s$ where K_u^a and K_u^s are the induced anisotropies related to the local anisotropy of the octahedral-icosahedral and trigonal-type clusters, respectively. The number of trigonal clusters varies as a function of P_{Ar} and thus explains the variation of K_u with P_{Ar}. In Co-Zr-Pt an extra contribution to K_u is observed due to the pseudodipolar ordering that results from the magnetic polarization of Pt. Co-Zr-Pt films exhibit a peculiar thermomagnetic relaxation that is explained by the reversibility of the pseudodipolar anisotropy and the thermal instability of trigonal-type clusters resulting from the substitution of Pt.

I. INTRODUCTION

Amorphous Co–nonmagnetic-transition-metal (M = Zr, Nb, Ti, Hf, etc.) thin films are currently being investigated[1–5] because they present attractive magnetic properties for use in magnetic recording technology as magnetic heads.[4,5] Indeed, by adjusting the composition one can easily produce films which exhibit a high saturation magnetization, a low coercive field H_c, and a negligible magnetostriction λ_s.[6] The production of material[1,5,7] with high permeability at high frequency requires the films to exhibit a small but well-defined in-plane uniaxial anisotropy field $H_k=2K_u/M_s$. Generally the preparation was performed by sputtering and on the as-deposited films a uniaxial anisotropy H_k was detected, which formed either spontaneously or by applying a magnetic field during the deposition. In spite of substantial efforts the physical origin of K_u is far from being understood until now. It was proposed that it could be related to some thermally induced pseudodipolar interaction via a pair ordering process.[8–12] Several authors pointed out also that the magnitude of K_u is unusually high if it is related to a monoatomic directional order.[13,14]

Recently, we reported a systematic study of the induced anisotropy[15–17] performed on amorphous $Co_{100-x}Ti_x$ thin films. It revealed that the pressure of the sputter gas P_{Ar} is the most important deposition parameter because the magnitude of K_u depends upon it. Effectively, for a given composition, K_u follows a bell-shaped variation as a function of P_{Ar}.[15] K_u was minimum $(K_u)_{min}$ for the lowest pressure used and exhibited a well-defined maximum $(K_u)_{max}$ for a critical pressure $(P_{Ar})_{crit}$. This result was explained by a model based on structural investigations.[16] The structure of amorphous $Co_{100-x}Ti_x$ thin films was interpreted as a random continuous matrix of sites with icosahedral, octahedral (fcc-like), and trigonal (hcp-like) symmetries.[17] The films deposited at the lowest pressure are built up essentially of icosahedral and octahedral clusters, which explain that the value of K_u is minimum. The variations of K_u with P_{Ar} are related to the evolution of the local structure via the variation of the amount and orientation of the trigonal type clusters. $(K_u)_{max}$ corresponds to an octahedral-trigonal phase transformation and now the contribution of the local anisotropy of trigonal clusters to K_u is maximum. In a previous work, we suggested that $(K_u)_{min}$ could be related to some pseudodipolar-type interaction. However, this last question remained basically open.[16]

The work reported in the present paper is an extension of the previous one to amorphous $Co_{95-x}Zr_5M_x$, M = Zr, Nb, Ti, and to $(Co_{91-x}Pt_x)Zr_9$ thin films. The investigations of the magnetic properties showed clearly that, in carefully prepared samples, experimental variations of $(K_u)_{min}$ as a function of concentration cannot be explained by a pseudodipolar mechanism. We also established some well-defined correlation between the observed

variations of K_u, that of the local structure, and the nature and concentration of M. Using these data we propose a model where K_u is the sum of two contributions $K_u^a + K_u^s$. K_u^a and K_u^s are related to the local anisotropies of sites with octa/icosahedral and trigonal-type symmetries, respectively. In Pt-substituted films, a supplementary contribution to K_u is observed, related to the induced moment developed by Pt. The results obtained by the thermomagnetic treatment strengthen also the as-proposed model.

The structure of the paper is the following. After a short recall of the experimental procedure the data are presented under five major headings as follows: The magnetic properties of amorphous CoZrM and CoZrPt alloys, the results of the structural investigations, the as-proposed model for K_u, and the discussion of the experimental data. Finally, the structural relaxation phenomena are described and the results of the thermomagnetic treatment are given.

II. EXPERIMENTAL PROCEDURE

The films were deposited by rf diode sputtering with Ar as a sputtering gas. In order to obtain the films with the desired composition, we used composite targets. It is formed of a vacuum melted target of composition $Co_{95}Zr_5$ on which triangular plates of corresponding metals were disposed in a regular way. The composition of the target is related to the lowest critical Zr concentration needed ($x_{min} \simeq 5\%$ at. Zr) for the obtainment of an amorphous phase. The concentration range investigated was typically $0 \leq x \leq 12$ for $Co_{95-x}Z_5M_x$ (M = Zr, Nb, Ti) and $5 \leq x \leq 10$ for $Co_{91-x}Zr_9Pt_x$. The magnetic and structural properties were examined on films deposited at P_{Ar} in the range $2\times10^{-3} \leq P_{Ar} \leq 15\times10^{-3}$ Torr. Unless otherwise stated, the rf power used was $W_{rf}=200$ W, corresponding to a deposition rate of $\simeq 2$ Å/sec. Other details are reported in Refs. 16 and 17.

The in-plane uniaxial anisotropy K_u was induced by performing the deposition process in a magnetic field of 700 Oe and using a substrate holder with a special configuration, the characteristics of which are reported in Ref. 8. It allows a minimum heating of the substrate surface so the deposition temperature is closed to 20 °C. K_u was determined on films of thickness in the range 0.25 ± 0.05 μm. The magnetic properties were investigated by vibrating-sample magnetometer (VSM), in-plane hysteresis B-H loop tracer working at 50 Hz, and ferromagnetic resonance (FMR) performed at $f=9.8$ GHz.

The structural and morphological studies were carried out on 0.04–0.08 μm-thick films deposited onto carbon-coated grids in a JEOL 200CX electron microscope. The microstructure was studied by transmission electron microscopy (TEM) in bright (BF) and dark (DF) fields. The structural state was explored by a transmission electron-diffraction pattern (TEDP). The TEDP profiles were traced by using a microdensitometer and resolved up to $s=2\sin\theta/\lambda=1.25$ Å^{-1}, where s is the scattering vector.

III. MAGNETIC PROPERTIES: $4\pi M_s$, H_c, AND K_u

A. $Co_{95-x}Zr_5M_x$ (M = Zr, Nb, Ti) thin films

In Fig. 1, the variations of $4\pi M_s$ are reported for the different alloys containing Zr, Nb, and Ti, respectively. The average magnetic moment per alloy atom $\bar{\mu}$ decreases linearly with increasing M concentration in agreement with previous investigations and with the theoretical expectations of the Friedel virtual bound-state model. The slope of the variation is fairly close to the theoretically expected one, i.e., $d\bar{\mu}/dc=-5$ (here $c=x/100$). However, some fluctuations of $\bar{\mu}$ as a function of the metal M are observed, its overall variations can be fitted by the expression

$$\bar{\mu}=[1.65-4.9c(\mathrm{Zr})-5.25c(\mathrm{Ti})-5.4c(\mathrm{Nb})]\mu_B \ . \quad (1)$$

In the as-deposited state, the coercive field H_c depends upon the deposition parameters and on M. H_c increases when the P_{Ar} used is higher and decreases when the rf input power W_{rf} or the deposition rate is increased. The value of H_c decreases when the amount of M in the deposit increases. For a given concentration H_c is the larg-

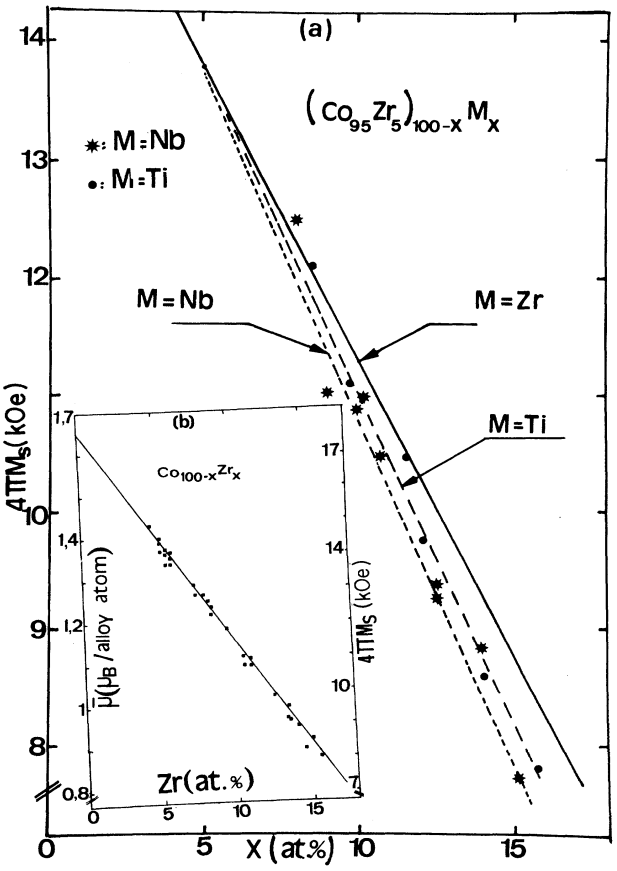

FIG. 1. (a) Saturation magnetization $4\pi M_s$ vs concentration for the alloys $Co_{95-x}Zr_xM_x$ with M = Zr, Nb, or Ti. (b) Magnetic moment per alloy atoms $\bar{\mu}$ for $Co_{100-x}Zr_x$ films.

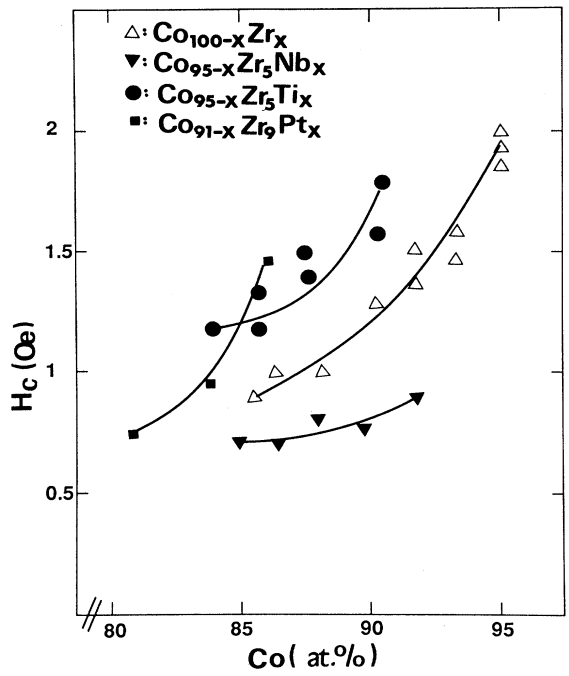

FIG. 2. Coercive field H_c vs concentration for the various alloys.

est and the smallest, respectively, for M = Ti and Nb (Fig. 2).

In Figs. 3(a)–3(c), the variations of K_u in $Co_{95-x}Zr_5M_x$ for M = Zr, Nb, and Ti, respectively, as a function of the pressure of the sputter gas are reported. The trends of variation are the same for the three alloys and like that observed on CoTi amorphous films. For a given composition K_u exhibits a bell-shaped variation as a function of P_{Ar}. K_u is minimal, $(K_u)_{min}$, for the lowest pressure used, it exhibits a well-defined maximum, $(K_u)_{max}$, for a critical pressure $(P_{Ar})_{crit}$ and it decreases for pressures higher than $(P_{Ar})_{crit}$. The critical pressure is the same whatever the composition is of the deposit and is in the range 8–9 mTorr.

In Figs. 4(a) and 4(b) are reported, respectively, the dependence of $(K_u)_{min}$ and $(K_u)_{max}$ on the concentration in M. The trend of variations of $(K_u)_{max}$ and $(K_u)_{min}$ are the same: Both terms decrease continuously when the M concentration in the film increases. The nature of the metal substituted for M affects the absolute value of K_u. At a given concentration x, $(K_u)_{min}$ is minimal for M = Nb and $(K_u)_{max}$ is maximal for M = Ti. The proposed model will allow us to explain these results.

B. $Co_{91-x}Zr_9Pt_x$ thin films

The variations at room temperature of the saturation magnetization $4\pi M_s$ as a function of Pt concentration are reported in Fig. 6(a). From this result the Bohr magneton per Co atoms $(\mu_B)_{Co}$ was computed which shows [Fig. 6(d)] that $(\mu_B)_{Co}$ increases with Pt dilution if one assumes that Pt is nonmagnetic. Our results are similar to previous observations and can be explained by band theory[19] or a model which involves localized moments on both Co and Pt.[20] We used the latter model where the results are explained that for this concentration range the moment of Co remains unchanged, while Pt develops an induced moment by its proximity with Co. Using this hypothesis the experimental results can be reasonably well fitted by the expression

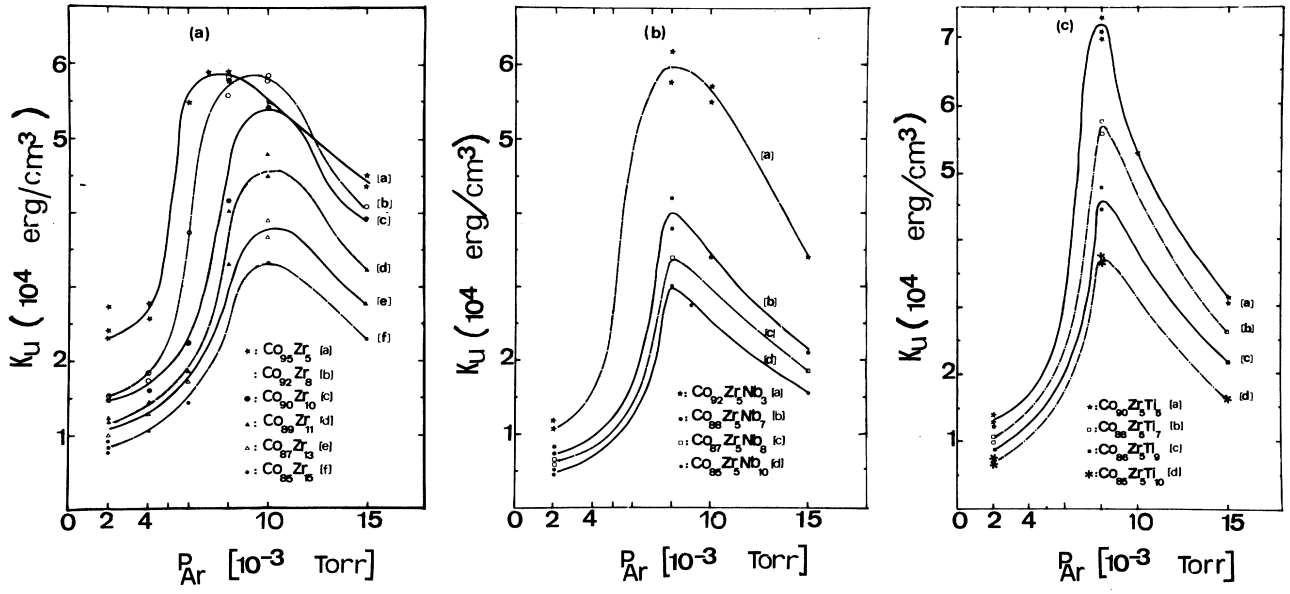

FIG. 3. Induced anisotropy K_u vs P_{Ar} in (a) $Co_{100-x}Zr_x$, (b) $Co_{95-y}Zr_5Nb_y$, (c) $Co_{95-y}Zr_5Ti_y$.

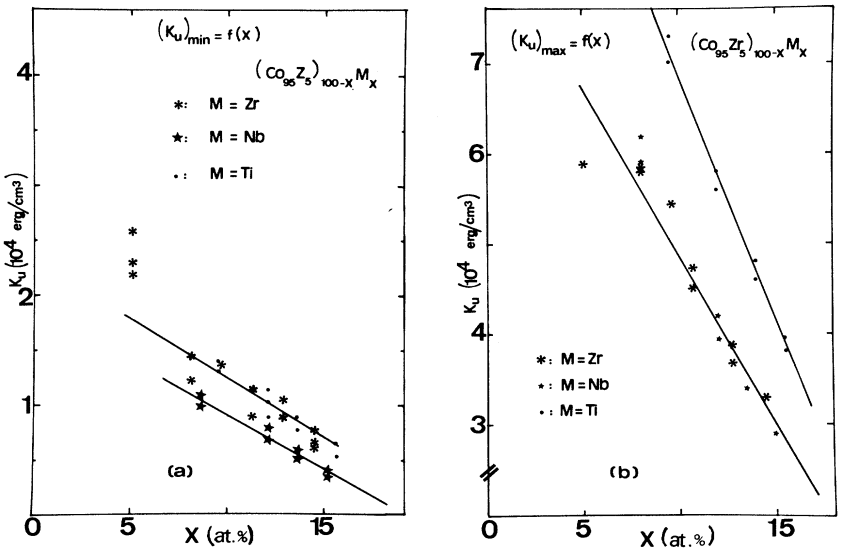

FIG. 4. Variations of (a) $(K_u)_{min}$ and (b) $(K_u)_{max}$ vs concentration in $Co_{95-x}Zr_xM_x$ alloys. $(K_u)_{min}$ and $(K_u)_{max}$ are defined in the Introduction.

$$(\bar{\mu}_B)_A = \bar{\mu}_B(1-c) + (\bar{\mu}_B)_{Pt}c \ , \tag{2}$$

where $\bar{\mu}_B = 1.23$ and $(\bar{\mu}_B)_{Pt} \simeq 0.4$. In expression (2) $(\bar{\mu}_B)_A$, $\bar{\mu}_B$, and $(\bar{\mu}_B)_{Pt}$ are the moment per unit alloy formula, per $Co_{91}Zr_9$, and per Pt, respectively.

The variations of K_u as a function of P_{Ar} for three different concentrations of Pt are shown in Fig. 5. The trend of change of K_u with P_{Ar} is similar to that detected for the other alloys. However, both $(K_u)_{min}$ and $(K_u)_{max}$ increase [Figs. 6(b) and 6(c)] with increasing Pt concentration in the films. These variations are opposite to those observed for Co-Zr-M alloys. They are related to the modifications of the magnetic properties and that of

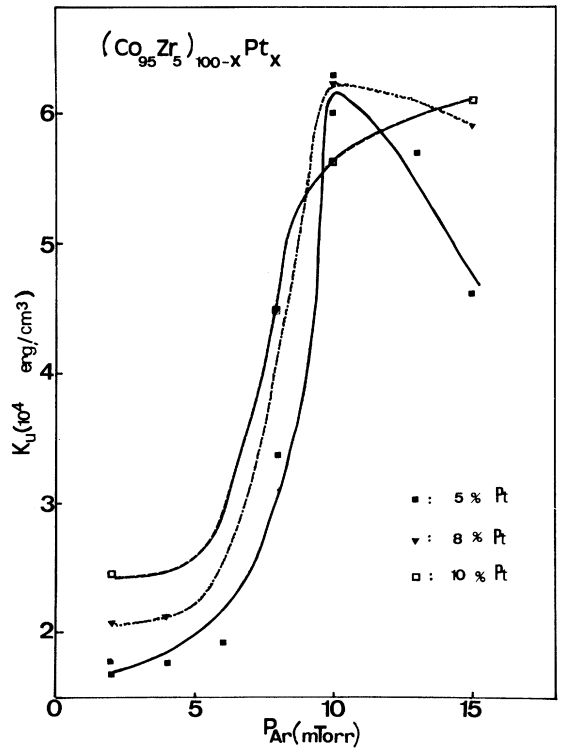

FIG. 5. K_u vs P_{Ar} in $Co_{91-x}Zr_9Pt_x$ films.

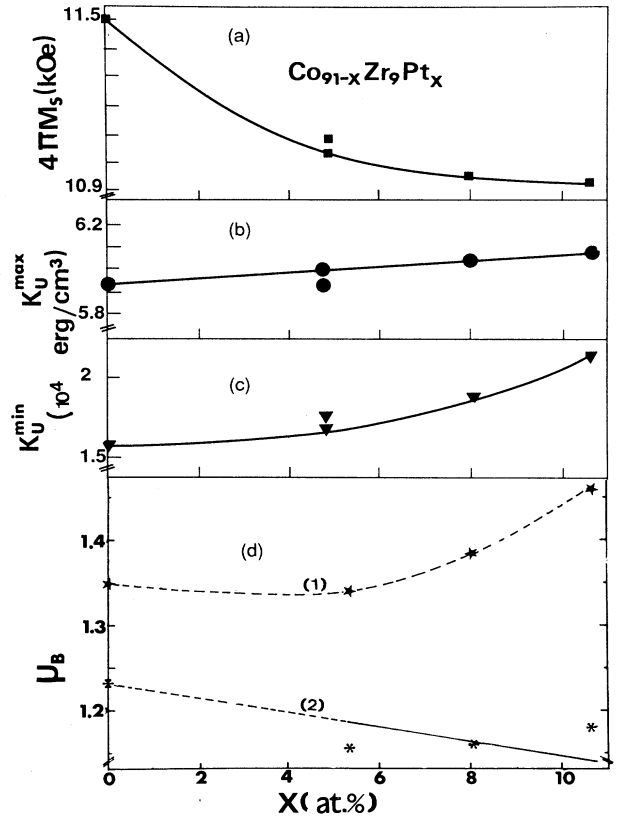

FIG. 6. Variations for $Co_{95-x}Zr_9Pt_x$ films of (a) $4\pi M_s$, (b) $(K_u)_{max}$, (c) $(K_u)_{min}$. The solid line is a calculated one using $(K_u)_{min} = K_u^a + Ax^2(1-x)^2$, (d) (1) magnetic moment $\bar{\mu}$ per Co atoms, (2) theoretical variations of $\bar{\mu}$ per alloy atoms by assuming that Pt is magnetically polarized.

the local structure generated by the substitution of Pt as will be shown in what follows.

IV. STRUCTURAL STUDIES: AS-DEPOSITED STATE

The structural investigations performed on Co-Zr-M films for M = Zr, Nb, and Ti revealed that these layers exhibit the same overall characteristics. The results will be illustrated by those obtained on $Co_{100-x}Zr_x$ films. The effect of pressure upon the structure was determined by studying systematically two sets of films deposited at 2 and 9 mTorr—so corresponding to $(K_u)_{min}$ and $(K_m)_{max}$—called hereafter the low-pressure (LP) and high-pressure (HP) samples, respectively.

The composition and the deposition conditions of the films investigated are reported in Table I. The TEM's obtained in BF and DF confirm that all these films elaborated at LP as well as HP were perfectly amorphous (Fig. 7). The TEM's corresponding to samples deposited at HP are more contrasted than those prepared at LP. This observation is similar to that reported by us on amorphous $Co_{86}Ti_{14}$ films and was discussed in Ref. 17.

The TEDP profiles corresponding to both LP and HP samples exhibit characteristics typical of the amorphous state: One detects broad and diffuse halos without contamination of Bragg peaks, a result in agreement with observations by TEM which did not reveal microcrystallites in DF. The overall profiles are similar to that obtained on a-$Co_{86}Ti_{14}$. However, the presence of Zr appears to favor the damping of the first broad and diffuse maxima and that of the shoulder on the second (Fig. 8).

The characteristics of the TEDP display some small but well-defined variations as a function of the nature of the metal M. When M is successively replaced by Ti, Nb, and Zr, one notes a more marked damping of the diffused intensities maxima, and a shift of the whole TEDP, hence the position s_1 and s_2 of the first and second maxima towards lower values of s. The shift obeys a linearly decreasing relationship of s_1 as a function of s_2 (Fig. 9), a result which corresponds to an expansion of the amorphous matrix. Such an effect could originate either from an increase of the free volume and/or an increase of the mean radial distance D_m between nearest-neighbor atoms. The contribution of each process can be estimated at least qualitatively by considering also Δs, which is the full width at half maximum of the first halo and characterizes the local disorder. In fact, generally Δs increases with increasing local disorder. Δs and D_m are smallest for M = Ti and largest for M = Zr, respectively (Figs. 10 and 11). One can conclude that when M is consecutively substituted by Ti, Nb, and Zr both the mean radial interatomic distance and the local disorder increase.

TABLE I. Sample numbering, composition, and preparation conditions of the films used for the structural study.

Sample number	Low pressure (LP) Composition	P_{Ar} (mTorr)	High pressure (HP) Composition	P_{Ar} (mTorr)
1	$Co_{86}Ti_{14}$	3 (Refs. 16,17)	$Co_{86}Ti_{14}$	8
2	$Co_{91}Zr_5Ti_4$	2	$Co_{90.3}Zr_{5.2}Ti_{4.5}$	8
3	$Co_{91.5}Zr_6Nb_{2.5}$	2	$Co_{91.7}Zr_6Nb_{3.3}$	8
4	$Co_{90.5}Zr_{9.5}$	2	$Co_{90}Zr_{10}$	10
5	$Co_{86}Zr_9Pt_5$	2	$Co_{86}Zr_9Pt_5$	10
6	$Co_{81}Zr_9Pt_{10}$	2	$Co_{81}Zr_9Pt_{10}$	13

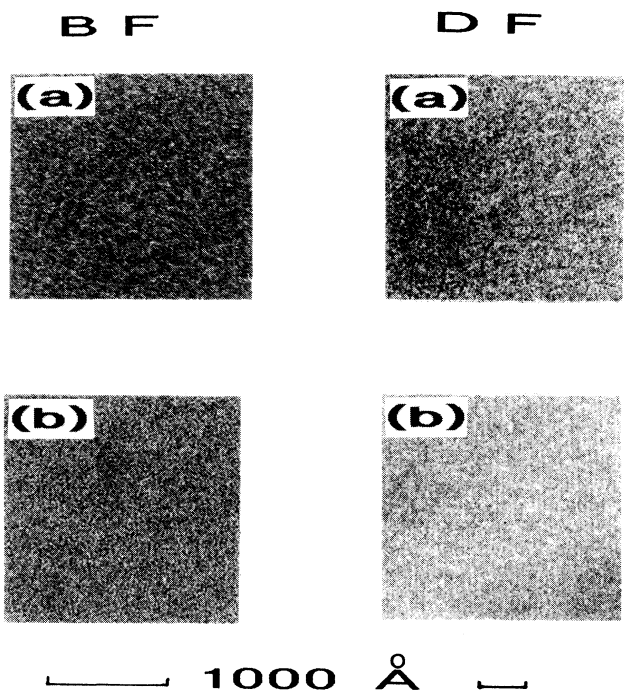

FIG. 7. BF and DF microstructure in Co-Zr films prepared at (a) high (HP) and (b) low pressure (LP). As-deposited state.

The TEDP profiles corresponding to Pt-substituted layers differ significantly from that observed on Co-Zr-M-type alloy films. An understanding of the results re-

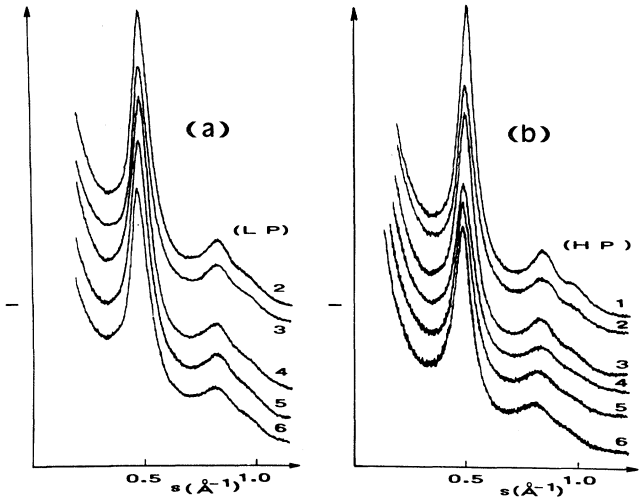

FIG. 8. TEDP profiles corresponding to thin films in the as-deposited state prepared at (a) LP and (b) HP (for numbering, see Table I).

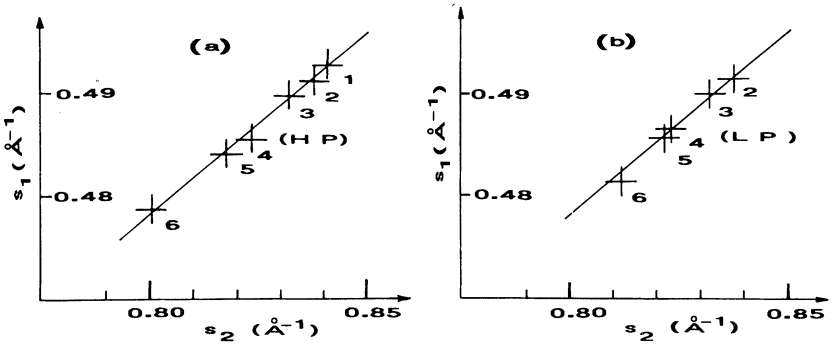

FIG. 9. Relationship deduced from the TEDP profiles of Fig. 8, between the locations s_1 and s_2 of the first and second maxima. Films prepared at (a) HP and (b) LP (for numbering, see Table I).

quires one to consider the role played by Pt and M in these alloys to be taken into account. General considerations and experiments about the glass-forming ability of metallic alloys show that in Co-rich Co-M alloys, M = Zr, Nb, Ti are to be considered as the glass-forming elements because of their large atomic size as compared to that of Co. On the other hand, the radius of Pt is much smaller than that of M's and Co-Pt form a fcc solid solution for the whole concentration range. Both effects are highly unfavorable phenomena for glass formation. Indeed no amorphous binary Co-Pt alloy could be obtained until now. Consequently, Pt has to be considered as a substitutional atom for Co. One can conclude that the as-observed structural changes should be explained by comparing the structural properties of $(Co_{91-y}Pt_y)Zr_9$ with those of $Co_{91-x}(Zr_5M_x)$, $x \simeq 5$, so the amount of the glass-forming atoms ($\simeq 9\%$ at.) in all samples is the same (Table I).

The TEDP in a-$(Co_{95-x}Pt_x)Zr_9$ films shift to lower values of s when the amount of the Pt content in the film increases (Fig. 9). This result can be explained if we accept that Pt has the same behavior in a-(CoPt)Zr films as it does in the fcc Co-Pt solid solution. The lattice parameter "a" of the fcc solid solution increases with increasing Pt content. Consequently, it should also produce an increase of D_m. This expansion can be characterized by $\Delta D_m/D_m$ and $\Delta a/a$, respectively, which indeed appears to be of the same order of magnitude in agreement with results reported in Table II. One can conclude that increasing the Pt substitution results essentially in an expansion of the amorphous network and hence that of D_m, while the local disorder decreases slightly. Indeed, the value of Δs is slightly smaller in $(CoPt)_{91}Zr_9$ as compared to that obtained in $Co_{90}Zr_{10}$ (Fig. 10).

The present interpretation can also be justified if one considers the variations of D_m as a function of $\delta = (R_{Zr,M})/(R_{Co,Pt})$. Here δ represents the size effect of the glass-forming atoms and, the greater its value, the more important the amorphization process. $(R_{Zr,M})$ and $(R_{Co,Pt})$ correspond to the mean radii of the (Zr, M) and (Co,Pt) atoms and were calculated from the composition. For an alloy of composition $(Co_{1-z}Pt_z)_{100-x}(Zr_{1-y}M_y)_x$,

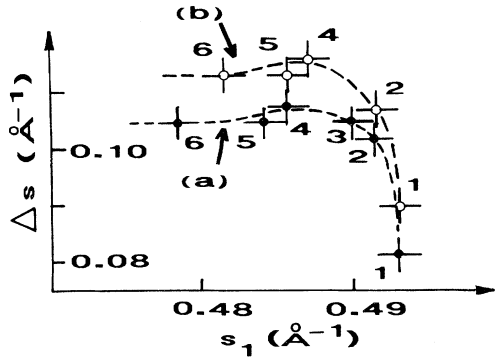

FIG. 10. Full width at half maximum Δs of the first maximum as a function of its position s_1 deduced from the TEDP profile of Fig. 8. Films prepared at (a) HP and (b) LP (for numbering, see Table I).

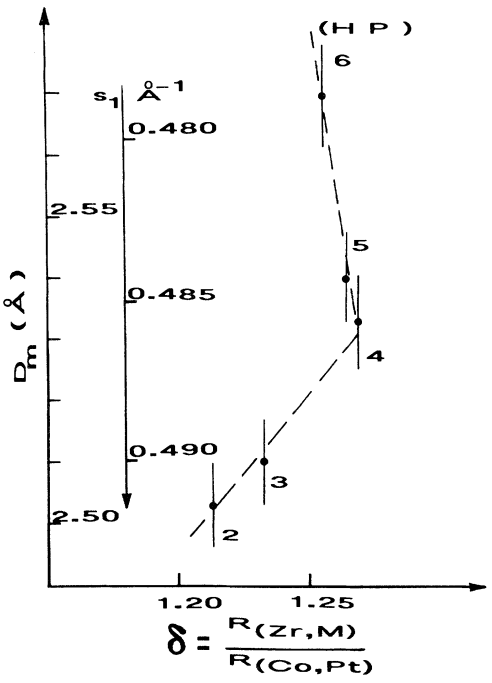

FIG. 11. Mean radial distance $D_m = 1.23/s_1$ as a function of $\delta = R_{Zr,M}/R_{Co,Pt}$, as deduced from the localization s_1 of the first maxima of the TEDP profiles (Fig. 8). $R_{Zr,M}$ and $R_{Co,Pt}$ are the mean radii of the (Zr,M) and (Co,Pt) atoms. The results correspond to HP films.

TABLE II. Reported results.

fcc solid solution (CoPt) of parameter a (Ref. 33)			Amorphous (Co, Pt)$_{100-x}$Zr$_x$ films deposited at (HP)		
Pt (at. %)	$\Delta a/a$ (%)	$\Delta D_m/D_m$ (%)	$D_m \pm 0.007$ Å	Pt (at %) (Co+Pt) (at. %)	Composition
0	0	0	2.533	0	$Co_{90}Zr_{10}$
5.5	0.37	0.3±0.5	2.540	5.5	$(Co_{86}Pt_5)_{91}Zr_9$
11.0	0.93	1.4±0.5	2.569	11.0	$(Co_{81}Pt_{10})_{91}Zr_9$

one has

$$R_{Zr,M}=(1-y)R_{Zr}+yR_M \ , \tag{3}$$

$$R_{Co,Pt}=(1-z)R_{Co}+zR_{Pt} \ . \tag{4}$$

Results reported in Fig. 11 show effectively that D_m increases linearly with $\delta=(R_{Zr,M})/R_{Co}$ indicating that the local disorder should increase when M is successively replaced by M = Ti → Nb → Zr. This result agrees with the experimental variation of Δs (Fig. 10). Conversely, in amorphous (CoPt)Zr thin films, D_m increases linearly with diminishing $\delta=R_{Zr}/R_{Co,Pt}$, while the local disorder decreases for higher Pt content (Fig. 10). One can conclude that these results also confirm the suggested effect of Pt upon the local structure.

More information about the changes of local structure as a function of P_{Ar} can be obtained by comparing the value of Δs exhibited by LP and HP films of like composition. Δs is systematically larger for LP films with respect to that detected for HP films showing that the local disorder of the first group is more marked, so present a better amorphization.

V. MODEL FOR THE ORIGIN OF K_u: DISCUSSION OF THE EXPERIMENTAL RESULTS

In an amorphous thin film the mechanism leading to the uniaxial anisotropy K_u can include several contributions which occurs at an atomistic or macroscopic level. Let us consider first K_u in the $Co_{95-x}Zr_5M_x$ films. A macroscopic origin of the induced anisotropy like that involving macroscopic stress via magnetoelastic effect, or anisotropically shaped heterogeneities (like voids) can easily be eliminated. No correlation was observed between the concentration dependence of λ_s (Ref. 13) and that of $(K_u)_{min}$ or $(K_u)_{max}$. Anisotropically shaped heterogeneities, in order to be effective, should be present with their largest dimension oriented along the direction of the applied field. Such defects were not detected by our structural investigations.

One can conclude that K_u is due to a microscopic process, so it is related to a directional chemical short-range order (CSRO) or to a topological short-range order (TSRO). When the induced anisotropy is related to the CSRO it involves a pseudodipolar-type anisotropy via a preferential distribution of atomic moment pairs.[22] In alloys containing only one type of magnetic atom, K_u is related to the monoatomic directional pair ordering. In agreement with theoretical formulas, if the Curie temperature of the alloys is high compared to the temperature of formation of K_u, which is the case here, the concentration dependence of K_u is given by $K_u \simeq Ax$, where $A \simeq$ const and x is the concentration of the nonmagnetic metal. In the present case the concentration dependence of $(K_u)_{min}$ is the reverse of the expected one. In effect, $(K_u)_{min}$ decreases with increasing x. The magnitude of K_u also differs from the presumed one. A theoretical computation[21] shows that K_u, in an amorphous alloy with a single kind of magnetic atom, should be of the order of $(2-4)\times 10^3$ erg/cm^3, in accordance with experimental data obtained on amorphous transition-metal–metalloid-type alloys like FeB, FePPb, or CoB.[22,23] $(K_u)_{min}$ is almost an order of magnitude larger than these values. Finally, if K_u is related to a CSRO it is at least a partially reversible process when submitted to a thermomagnetic treatment. As will be shown in Sec. VII, this was not the case here. All these results are very strong arguments to eliminate a pseudodipolar-type anisotropy as the basic mechanism for the origin of K_u.

The conclusion is that K_u should be related to the TSRO and the model that we propose is the following: In Co-Zr-M thin films the field-induced anisotropy K_u involves the single-ion anisotropy via local spin-orbit coupling. The magnitude of spin-orbit coupling is related to the local configuration, so K_u is a structural anisotropy and is the sum of two contributions:

$$K_u=K_u^a+K_u^s \ . \tag{5}$$

K_u^s is the induced anisotropy related to the local anisotropy K_l^s corresponding to Co atoms in trigonal clusters and K_u^a to the local anisotropy K_l^a corresponding to Co atoms in octahedral and/or icosahedral clusters. The contribution of K_u^s to K_u is negligible on films deposited at the lowest pressure. This assumption is confirmed by the thermomagnetic relaxation process (see Sec. VII). Consequently one has

$$(K_u)_{min}=K_u^a \ . \tag{6}$$

Based on this model we propose the following mechanism for the formation of K_u. The film is saturated along the applied field during its formation. Local rearrangement of the atoms tends to occur in order to minimize the magnetic energy. Consequently, the spatial distribution of the clusters is no longer isotropic but a certain amount with their easy axis will be oriented preferentially parallel to the applied field. This reordering can occur by

various mechanisms like diffusion via jump of atoms or by diffusionless local structural transformation. The amount of the nonmagnetic transition metal M is relatively small and its atomic radius is large so a process based upon the diffusion of M is quite unlikely. Diffusionless transfiguration involving transformation of icosahedral to octahedral clusters was proposed for a similar amorphous compound.[24] It was also shown that the energy difference between these two configurations is quite small,[24] which is also evidence in favor of this process.

The value of K_u^a varies as a function of the film composition as expected, but independent of the P_{Ar} used during the deposition. This result can be explained using the following assumptions: For a given composition the value of K_u^a is governed by the deposition temperature of the films, the magnitude of K_l^a during its formation, and the free volume. The temperature of the substrate remains close to room temperature whatever P_{Ar} is.[18] Consequently, K_l^a is also independent of the deposition parameters. The variation of the free volume with P_{Ar} is sufficiently small, so as not to affect the magnitude of K_u^a.

Within the framework of the proposed model the relationship between the induced and local anisotropies is given by

$$(K_u)_{\min}=K_u^a=K_l^a\sum_i C_i \tag{7a}$$

and

$$(K_u)_{\max}=K_l^a\sum_i C_i+K_l^s\sum_{il} C_{il}' \ , \tag{7b}$$

where C_i and C_i' are the concentration of the ith orientation clusters, with C_i corresponding to the icosahedral-octahedral and C_i' to the trigonal type. The local anisotropies K_l^a and K_l^s are a function of two parameters: the local symmetry seen by the Co atoms and of M_s. In agreement with structural investigations, the local disorder increases, so the octahedral and the trigonal-type clusters are less well defined when the x content in the film increases. This mechanism should affect, in particular, the trigonal-type clusters. Theoretical expectation predicts[25] that if the local anisotropy is of single-ion type, one has $K_l \sim M_s^{\lambda}$ with $\lambda \sim 1$. Both parameters generate a decrease of K_l^a and K_l^s for increasing x content.

The value of K_l^a and its concentration dependence could be deduced in $Co_{100-x}Zr_x$ films from the characteristics of the standing spin-wave spectra[26] and exhibit the expected behavior [Fig. 12(a)]. Using these values of K_l^a one can estimate the amount of the clusters C_i affected by the reordering process. In this process the easy axis of the clusters tends to lie parallel to the magnetic field applied during deposition. C_i increases rapidly with x as shown in Fig. 12(b). This variation also agrees with the expected one. The probability for a cluster to be reordered depends on the local composition. Clusters formed of only Co atoms are magnetically isotropic, while those where the Co atoms possess M atoms as nearest neighbors present a net local anisotropy, so submitted to greater energy. The free volume, which increases with increasing x content, could also favor the reorientation process. One can conclude that the decreases of both $(K_u)_{\min}$ and $(K_u)_{\max}$ as a function of the increasing amount of x content are related to the decrease of the magnitude of K_l^a and K_l^s. This outcome remains unbalanced by the enhanced amount of favorably oriented clusters, hence the as-observed data.

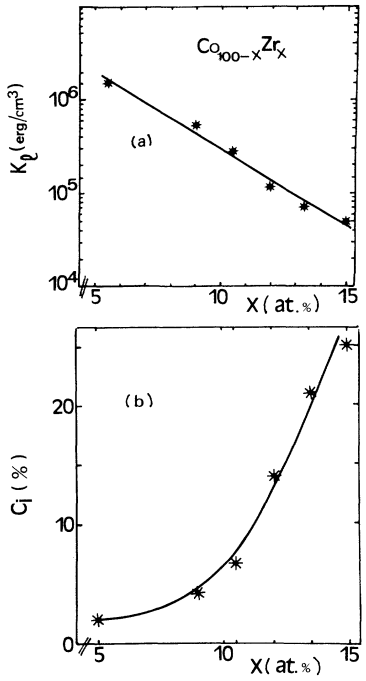

FIG. 12. (a) Variations of the random local anisotropy K_l^a vs concentration x for $Co_{100-x}Zr_x$ films as deduced from standing-spin-wave spectra (Ref. 26). (b) Amount of as-calculated concentration of clusters C_i (in %) oriented with their easy axis along the easy anisotropy axis of the film.

The peculiar effect of the various substitution for M upon K_u are also related to a change in the values of K_l. For a given composition $(K_u)_{\min}$ is the smallest for M = Nb. In the concentration range investigated λ_s is smaller in Co-Zr-Nb films compared to the two other alloys of the same composition. Consequently, one can assume that the magnitude of K_l^a is also smaller. In $Co_{95}Zr_5$ films, e.g., when the composition approaches the ordered crystalline state, the value of $(K_u)_{\min}$ increases substantially compared to layers with higher Zr content. This result also confirms the strong influence of local atomic arrangement upon the value of K_l^a. The values of $(K_u)_{\max}$ for a given concentration are systematically higher for M = Ti than for M = Nb or Zr. This outcome is in agreement with structural investigation which showed that the local disorder is significantly smaller so the value of K_l^s is higher in Ti-substituted layers as compared to the two others.

In the (CoPt)Zr thin films, the concentration dependence of $(K_u)_{\min}$ and $(K_u)_{\max}$ is markedly different from that detected for Co-Zr-M alloys. These results are related to the magnetic state of Pt, and the modification of the local structure as induced by the substitution of Pt. The

Pt atoms being magnetically polarized, the (CoPt)Zr films have to behave as magnetically diatomic alloys. Hence this should result in a contribution of a diatomic pseudodipolar directional ordering process to $(K_u)_{\min}$. Indeed the experimentally observed variations of $(K_u)_{\min}$ can be nicely fitted [Fig. 6(c)] by the expression $(K_u)_{\min}=K_u^a+Ax^2(1-x)^2$, where K_u^a is the local anisotropy corresponding to the $Co_{91}Zr_9$ matrix and the second term is the usual expression corresponding to the diatomic pseudodipolar ordering.

As shown in Fig. 6(b) $(K_u)_{\max}$ increases as a function of increasing Pt content in (CoPt)Zr films. Pt occupies a substitutional position (Sec. IV) resulting in an extension of the network and a decrease of the local disorder. Consequently, the trigonal clusters are structurally better defined. Moreover, M_s decreases only slightly with increasing Pt concentration. Both mechanisms contribute to the result obtained.

VI. STRUCTURAL-RELAXATION PHENOMENA

The structural evolution as a function of an annealing treatment was observed via *in situ* electron microscopic studies. It allowed us to determine the thermal stability of the films and facilitated the understanding of the thermomagnetic relaxation process. The influence of the deposition parameters upon the structural relaxation was determined by comparing LP and HP films of the same composition. The experiments consisted of submitting the films to an isothermal heat treatment in the electron microscope, in steps of 50 °C. After holding them at the annealing temperature for 10 min, they were quenched down rapidly to room temperature where the investigations were performed.

The structural relaxation process occurring on the Co-Zr-M systems is illustrated by the results obtained on $Co_{90}Zr_{10}$ HP and LP films. The diffusion profile corresponding to the HP layer (Fig. 13) exhibits a first and a second maxima resolved better and a shoulder more marked after an annealing at 250 °C. This evolution indicates that as a result of the annealing the local order is extended to longer distances. Moreover, at this temperature the film remained amorphous as no microcrystals could be detected on the DF micrography. A primary crystallization of fcc Co occurs at $T_{Cr}\cong 300$°C (Ref. 27) in the Zr-enriched amorphous Co-Zr matrix. The overall process is the same in LP films. However, now $T_{Cr}\cong 250$°C, a result which confirms that T_{Cr} is significantly lower in LP films as compared to HP ones.

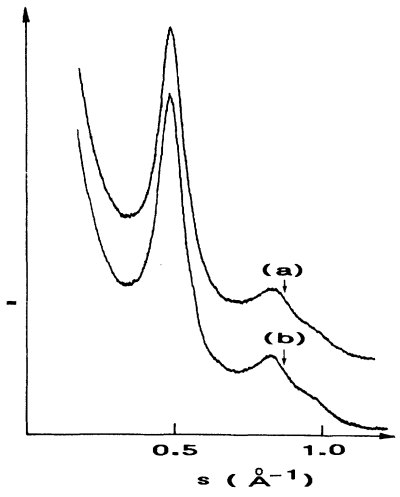

FIG. 13. TEDP profiles of $Co_{90}Zr_{10}$ films prepared at HP (a) as-deposited and (b) annealed at 250 °C.

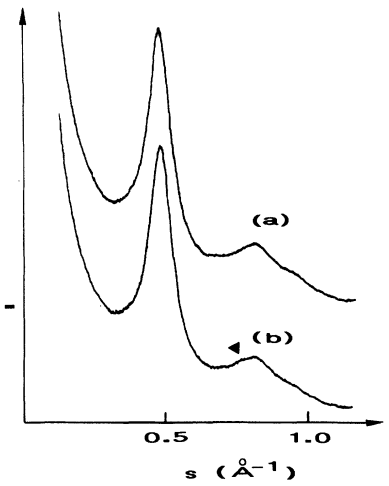

FIG. 14. TEDP profiles of $(Co_{81}Pt_{10})Zr_9$ films prepared at (HP) (a) as-deposited and (b) annealed at 250 °C.

The effect of substitution of Co by Pt on the relaxation was observed on films of composition $(CoPt)_{91}Zr_9$. Both the LP and HP films remain amorphous for annealing performed up to 300 °C, but the observed change of the diffusion spectra is fairly unusual: Effectively a widening of the diffusion maxima, a damping of the oscillations of the TEDP profile, and the appearance of another shoulder on the lower side of the second maximum near 0.75 $Å^{-1}$ occurs (Fig. 14). This result is characteristic of the formation of octahedral sites in the annealed film and can

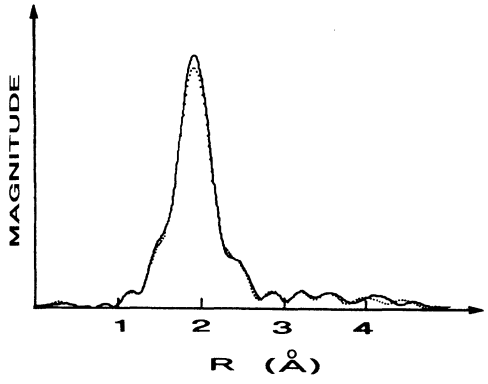

FIG. 15. Fourier transforms of the EXAFS spectra above the Co K absorption edge detected on $(Co_{81}Pt_{10})Zr_9$ films prepared at HP. (a) Dotted line, as-deposited state. (b) Solid line, sample annealed at 250 °C.

be explained in the following way: In its crystalline state the Co-Pt alloy exists only as a fcc solid solution. Consequently, in the amorphous phase only the octahedral clusters are thermally stable and the trigonal-type clusters which form as a result of the applied magnetic field during deposition are thermally highly unstable and transform easily to octahedral ones. This transformation conserves coordination number and interatomic distances between nearest neighbors. We tried to verify it in a study carried out by the extended x-ray-absorption fine-structure (EXAFS) technique on both the as-deposited and annealed $(Co_{90}Pt_{10})_{91}Zr_9$ HP films. The annealing was performed at 250 °C during 1 h. The spectra were recorded at 77 K above the Co K-edge absorption by the transmission mode. The Fourier transforms obtained from the two EXAFS data are reported in Fig. 15. The peak corresponding to the nearest neighbors occurs at the same radial distance and has almost the same area, but its intensity increased about 6% on the as-annealed film. It indicates clearly that on the annealed layer the local ordering is slightly better defined without a change of coordination number and interatomic distance between nearest neighbors, as expected.

As we pointed out above, both HP and LP $(Co_{90}Pt_{10})_{91}Zr_9$ films annealed up to 300 °C are amorphous as opposed to the two sets of Co-Zr films. Now T_{Cr} is 320 and 350 °C for the LP and HP (CoPt)Zr layer, respectively. This result indicates that the thermal stability of the amorphous state is higher in (CoPt)Zr alloys as compared to Co-Zr ones.

VII. THE THERMOMAGNETIC RELAXATION PROCESS

The thermomagnetic annealing was performed in a transverse magnetic field of $\simeq 500$ Oe and under a vacuum of 5×10^{-7} Torr. The variations of K_u were studied in isothermal annealing experiments as a function of time. The films were heated at a rate of ~ 40°C/min, maintained at the annealing temperature which was in the range 100–300 °C, and then cooled rapidly down to room temperature (~ 150 °C min^{-1}). The variations of K_u were deduced from the study of the hysteresis loop and also controlled by FMR. No preannealing was performed, so the progressive elimination of the free volume could affect the relaxation rate in the first steps of the annealing.

Let us consider the relaxation phenomena in Co-Zr-M thin films. The main experimental results are reported in Figs. 16 and 17. The time-dependent relaxation process, as obtained on a typical set of films of the same composition but deposited at various pressures, is shown in Fig. 16(a). After a first period, where K_u decreases sharply on all samples, a second stage occurs. Now the behavior of the film is related to the pressures used during its forma-

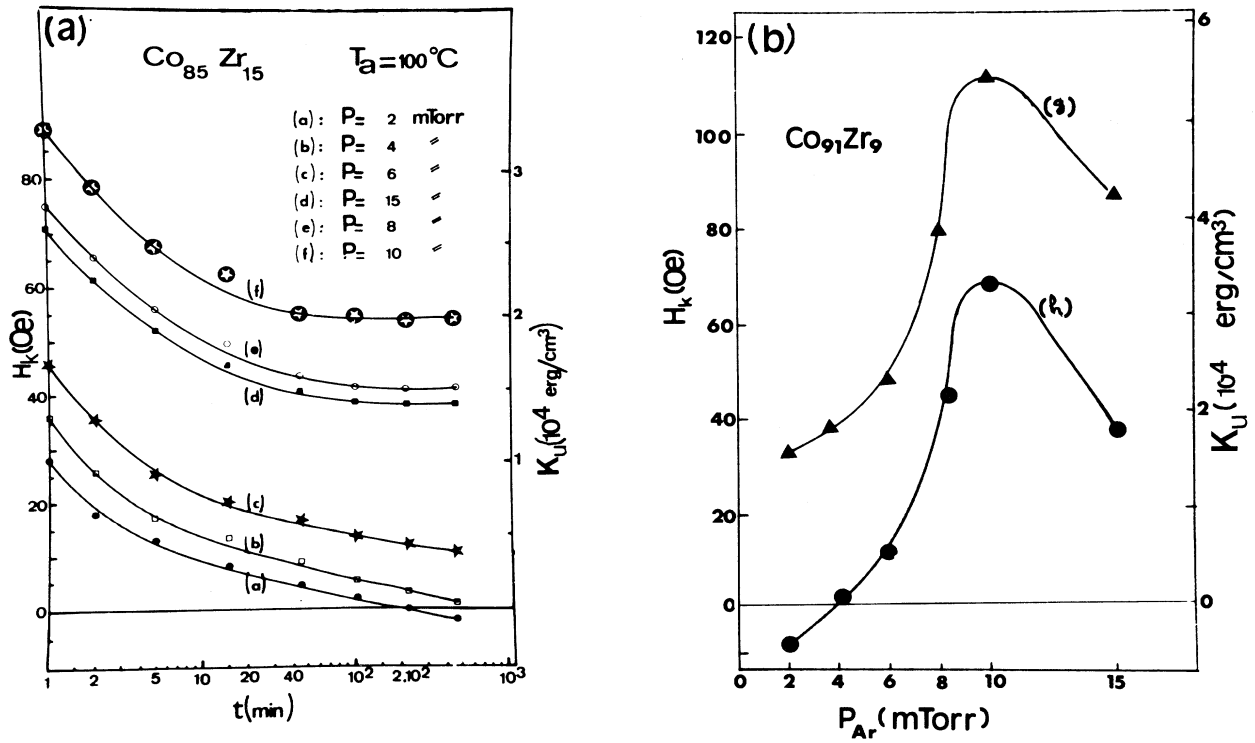

FIG. 16. (a) Thermomagnetic relaxation of K_u as a function of time performed at an annealing temperature $T_a = 100$ °C. (b) As-deposited (g) and residual value (h) of $H_k - (H_k)_{res}$, for $Co_{91}Zr_9$ films deposited at various pressures P_{Ar}. $(H_k)_{res}$ was obtained for $T_a \simeq 300$ °C and $t = 30$ min.

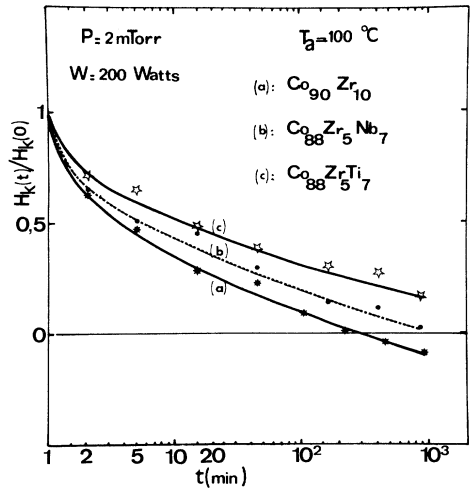

FIG. 17. Thermomagnetic relaxation of $H_k = 2K_u^a/M_s$ as a function of time. $H_k(0)$ correspond to the as-deposited state. The concentration in the three alloys Co-Zr, Co-Zr-Nb, and Co-Zr-M of the nonmagnetic transition metal is fairly closed.

tion. On films deposited at high pressures ($P_{Ar} \geq 8$ mTorr) K_u is practically unchanged, while on those prepared at $P_{Ar} < 8$ mTorr K_u decreases fairly slowly. On the film prepared at the lowest pressure a small uniaxial anisotropy field is formed along the applied field after a fairly long annealing time. However, its amount is typically in the range $(2-3)\times 10^3$ erg/cm^3, which is an order of magnitude smaller than K_u^a obtained in the as-deposited state. Moreover, this value of the induced anisotropy field is practically independent of the concentration of the films. This result cannot be explained by too slow a diffusion rate.[29] Other investigations revealed a similar behavior of K_u in Co-Zr-M alloys. Yip *et al.*[30] reported that the energy required to induce an anisotropy field is several orders of magnitude higher than that necessary for its suppression. Fukanaga, Okabe, and Narita[31] found that the reorientation process of the magnetic anisotropy in $Co_{90}Zr_{10}$ is extremely slow.

These results show that K_u displays a basically irreversible behavior and is composed effectively of two contributions: A first one which can be suppressed by an annealing treatment performed at relatively low temperatures $(K_u)_{sup}$, and a second one having a much higher thermal stability. Each contribution can be easily identified as follows [Fig. 16(b)]: The magnitude of $(K_u)_{sup}$ which is the same on samples of identical composition, but deposited at various P_{Ar}, is close to $(K_u)_{sup} \simeq K_u^a$. The residual value of $K_u - (K_u)_{res}$ — is $(K_u)_{res} \simeq K_u^s$ so it corresponds to trigonal-type clusters, which explains that $(K_u)_{res}$ follows a bell-shaped variation [Fig. 16(b)]. This high thermal stability of trigonal-type clusters is confirmed both experimentally and theoretically. The magnitude of $(K_u)_{res}$ was practically unchanged even for annealing performed at 300 °C. Computation by Eberhardt, O'Handley, and Johnson[28] showed that pure Co was more stable in the hcp than in the fcc phase. They could conclude that clusters with trigonal symmetry are thermally more stable than octahedral ones.

The relaxation rate depends on the metal substituted for M. We determined it on samples deposited at 2 mTorr. It is the highest and the lowest for M = Zr and Ti (Fig. 17), respectively. As expected, it is governed by the free volume and the local disorder which, for a given concentration is greatest for M = Zr, results in agreement with those obtained by Machata, Tsunashima, and Vchiyama[32] who showed that the activation energy in a-CoM alloys is greatest for M = Zr.

The relaxation process observed on (CoPt)Zr thin films is different from that exhibited by Co-Zr-M alloys. The results are illustrated in Fig. 18 and can be summarized as follows. The thermal stability of K_u varies strongly with the P_{Ar} used and the Pt concentration. On films with high Pt concentrations, K_u can be completely suppressed even on samples deposited at pressures as high as $P_{Ar} = 10$ mTorr. The residual value of K_u does not correspond to K_u^s but is generally much smaller. Moreover, it depends strongly on the annealing temperature used. This comportment of K_u is related to the thermally unstable trigonal clusters which transforms easily to octahedral ones, so a large part of K_u^s can be easily suppressed by annealing. The relaxation rate is much faster, in particular in the initial stage, for Co-Zr-Pt thin films as compared to Co-Zr-M. K_u exhibits a fairly large reversible part, which increases continuously with increasing Pt content. These results are simply connected to the fact that a large portion of K_u originates from the pseudodipolar anisotropy, which displays a high

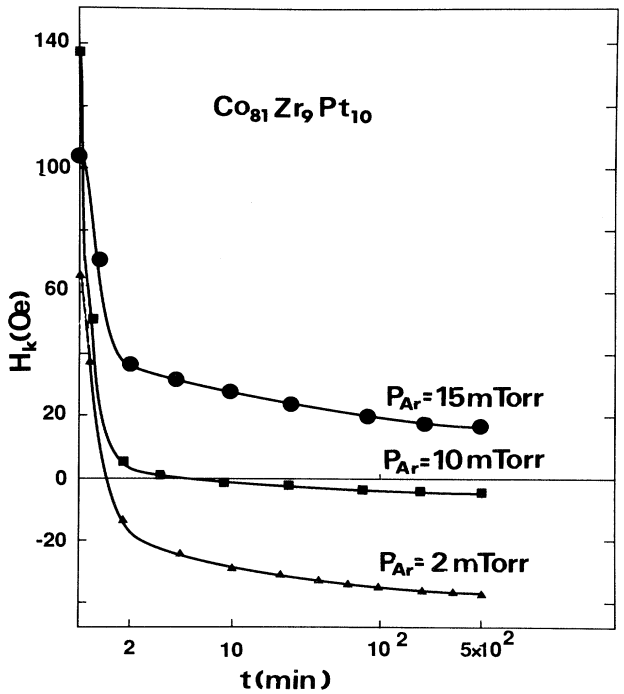

FIG. 18. Thermomagnetic relaxation of H_k as a function of time in $Co_{81}Zr_9Pt_{10}$ thin films deposited at various P_{Ar}. $T_a = 200$ °C.

activation energy and is essentially a reversible phenomenon.

VIII. SUMMARY AND CONCLUSIONS

We have performed a study on amorphous Co-Zr-M and Co-Zr-Pt thin films, with the aim to determine the physical origin of K_u. The variations of K_u as a function of the nature of the substituted metal were studied systematically and these results could be correlated with the evolution observed in the local structure. We developed a model where K_u is related to the local anisotropy of the various clusters formed during the deposition process and is the sum of two contributions related to octa/icosahedral and trigonal-type clusters, respectively. These two components of K_u can clearly be separated by an annealing experiment because they possess a substantially different thermal stability.

In Co-Pt-Zr, a pseudodipolar contribution to K_u could be clearly identified related to the pair ordering of a magnetically diatomic alloy. Consequently, the thermomagnetic relaxation of K_u becomes reversible. The present model allows us to also explain the unusually high value of K_u in a-CoZrM thin films, reported by the various experimenters.

ACKNOWLEDGMENTS

J. Sztern is gratefully acknowledged for help in the preparation of the samples. A. Sadoc from LURE performed the experiments by EXAFS. Laboratoire de Magnétisme is Unité Propre du CNRS. Laboratoire de Métallurgie is Unité Associée au CNRS No. 159.

[1]Y. Shimada, IEEE Trans. Mag. **MAG-22**, 89 (1986).
[2]K. Yamada, T. Maruyama, H. Tanaka, H. Kaneko, I. Kagoya, and S. Ito, J. Appl. Phys. **55**, 2235 (1984).
[3]Y. Kamo, S. Kikuchi, and Y. Shimada, J. Appl. Phys. **64**, 5673 (1988).
[4]H. Edelmann, IEEE Trans. Mag. **MAG-25**, 3194 (1989).
[5]J. L. Su, M. Chen, I. Lo, and R. E. Lee, J. Appl. Phys. **63**, 4020 (1988).
[6]H. Fujimori, N. S. Kazama, K. Hirose, J. Zhang, M. Morita, I. Sato, and H. Suganara, J. Appl. Phys. **55**, 1769 (1984).
[7]Y. Ochiai, M. Mayakawa, K. Mayashi, and K. Aso, J. Appl. Phys. **63**, 5424 (1988).
[8]H. Hoffman, G. Kellet, and K. H. Kammerer, IEEE Trans. Mag. **MAG-23**, 2731 (1987).
[9]H. Fukunaga and K. Narita, Jpn. J. Appl. Phys. **21**, L279 (1982).
[10]T. Takahashi, N. Ikeda, and M. Nave, J. Appl. Phys. **69**, 5011 (1991).
[11]M. Morita, Y. Fukushima, M. Yamomota, and J. Fujimori, J. Magn. Magn. Mater. **49**, 301 (1985).
[12]K. K. Choh, J. M. Judy, and J. M. Siverstein, IEEE Trans. Mag. **MAG-23**, 2539 (1987).
[13]H. J. de Witt, C. H. M. Witmer, and F. W. A. Dirne, IEEE Trans. Mag. **MAG-23**, 2123 (1987).
[14]Y. Shimada, and H. Kojima, J. Appl. Phys. **53**, 3156 (1982).
[15]G. Suran, K. Ounadjela, and F. Machizaud, Phys. Rev. Lett. **57**, 3109 (1986).
[16]K. Ounadjela, G. Suran, and F. Machizaud, Phys. Rev. B **40**, 578 (1989).
[17]F. Machizaud, K. Ounadjela, and G. Suran, Phys. Rev. B **40**, 587 (1989).
[18]K. Ounadjela, G. Suran, and J. Sztern, Thin Solid Films **151**, 397 (1987).
[19]A. R. Williams, V. L. Moruzzi, A. P. Malozemoff, and K. Terakura, IEEE Trans. Mag. **MAG-19**, 1983 (1983).
[20]A. R. Williams, A. P. Malozemoff, V. L. Moruzzi, and M. Matsui, J. Appl. Phys. **55**, 2353 (1984).
[21]P. Allia and F. Viai, IEEE Trans. Mag. **MAG-14**, 1050 (1978).
[22]T. Miyazaki and M. Takahashi, J. Magn. Magn. Mater. **42**, 29 (1984).
[23]F. E. Luborsky and J. L. Walker, IEEE Trans. Mag. **MAG-13**, 953 (1978).
[24]M. E. Eberhart, K. H. Johnson, D. Adler, R. C. O'Handley, and M. E. Mc Henry, J. Non-Cryst. Solids **75**, 97 (1985).
[25]E. M. Chudnovsky, W. M. Saslow, and R. A. Sirota, Phys. Rev. B **33**, 151 (1986).
[26]G. Suran, M. Naili, M. Rivoire, and J. C. S. Levy, J. Appl. Phys. **67**, 5849 (1990); G. Suran, M. Rivoire, and J. C. S. Levy, J. Magn. Magn. Mater. (to be published).
[27]The as-determined value of T_{Cr} is significantly lower than that deduced from differential scanning calorimetry or from resistivity measurements [see, for example, R. M. Idrus and P. J. Grundy, J. Phys. D **19**, 1245 (1986)]. However, direct microscopic observation is a much more sensitive probe for the determination of the structure.
[28]M. E. Eberhart, R. C. O'Handley, and K. H. Johnson, Phys. Rev. B **29**, 1097 (1984).
[29]H. Mehrer and W. Dörner, Defect Diffusion Forum **66-69**, 189 (1989).
[30]Y. Yip, M. J. Vois, M. Lu, M. P. Dugas, and J. H. Judy, IEEE Trans. Mag. **MAG-24**, 1109 (1986).
[31]H. Fukunaga, K. Okabe, and K. Narita, Jpn. J. Appl. Phys. **24**, 1109 (1986).
[32]Y. Machata, S. Tsunashima, and S. Vchiyama, IEEE Trans. Mag. **MAG-22**, 1107 (1986).
[33]W. B. Pearson, *A Handbook of Lattice Spacing and Structures of Metals and Alloys* (Pergamon, Oxford, 1964), Vol. 4, p. 519.

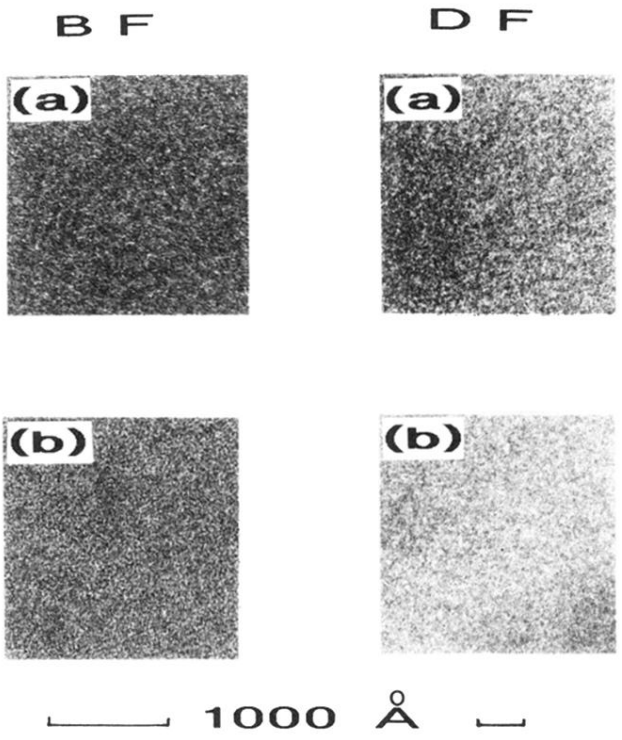

FIG. 7. BF and DF microstructure in Co-Zr films prepared at (a) high (HP) and (b) low pressure (LP). As-deposited state.